

# Communications

## Novel UHF RFID Tag Antenna for Metallic Foil Packages

Jeongki Ryoo, Jaeyul Choo, and Hosung Choo

**Abstract**—A low-cost wideband antenna for radio-frequency identification (RFID) tags for use with metallic foil packages is designed in this communication. An proximity inductively coupled feed structure is employed to perform wideband impedance matching between a slot on a metallic foil package and a small rectangular feeding loop connected to a microchip. The results show a measured half-power bandwidth of 32.2% (799 MHz–1,093 MHz) and a reading distance of over 10 m.

**Index Terms**—Low-cost, metallic foil package, UHF RFID tag, wide bandwidth.

### I. INTRODUCTION

In ultra-high frequency radio-frequency identification (UHF RFID) systems, the reader transmits a microwave signal to a tag that is composed of an antenna and a microchip. The microchip then responds to the reader using a modulated backscattered signal by varying its input impedance. The tag antenna in UHF RFID systems is one of the most important components, and should be able to overcome performance degradation caused by nearby dielectric or metallic materials. However, underlying metallic objects such as metallic foil packages are strong determinants of antenna impedance change, resulting in poor impedance matching and reduced reading distance. To overcome this problem, some tag antennas that can be mounted on metallic objects have been proposed [1]–[4]. Such antennas usually employ a thick dielectric inner layer between a tag and the metallic surface, and this bulky structure increases fabrication costs and restricts the range of applications. Recently some researchers have proposed a slot-type tag that uses the conducting surface of foil packaging as a slot radiator [5], [6]. These slot-type antennas are much more efficient than dipole-type antennas since the currents spread throughout the broad surface of the foil packaging sheet. However, a single slot antenna has a narrow bandwidth, and thus its radiating performance can be easily changed by dielectric objects in the foil packaging. Moreover, a single-slot tag antenna is not suitable for mass production due to the difficulty of directly connecting the microchip to a metallic foil package [5]–[7].

In this communication, we propose a novel inductively coupled slot antenna to be used with metallic foil packages. The tag antenna is composed of a slot radiator, which is made by cutting a slit in the metallic foil surface of the package, and a loop feeder, to which the tag chip is attached at the center. This inductively coupled feeding structure enables detuning of the resonant frequency and impedance without changing the slot dimensions in the packaging foil. In addition, the inductive

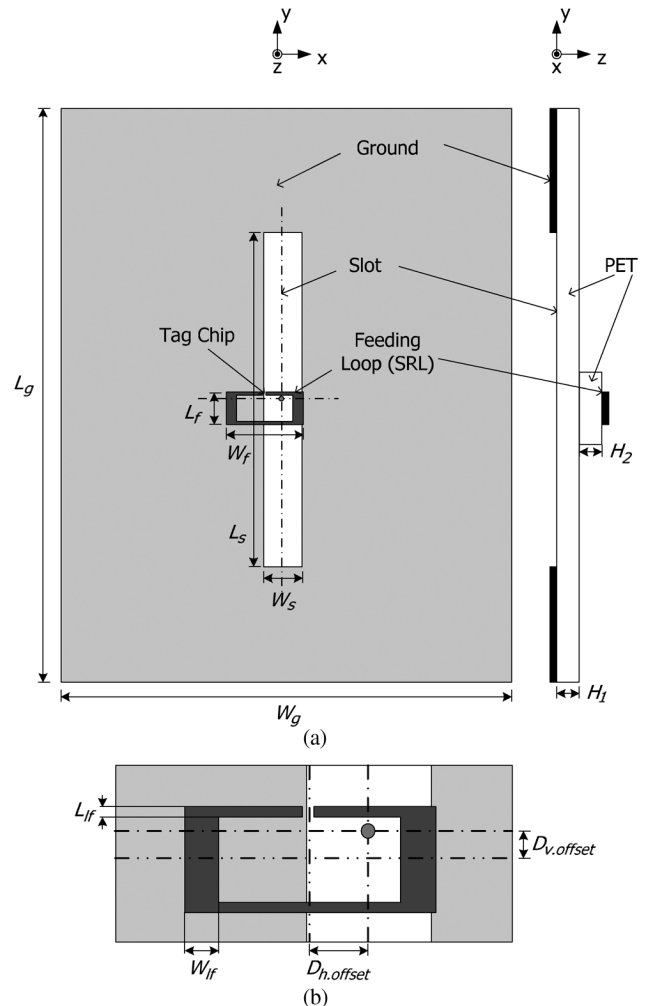


Fig. 1. Proposed RFID tag antenna structure: (a) configuration of the tag, (b) proximity inductively coupled feed structure.

coupling between the slot and the loop feeder provides a broadband property, and results in good impedance matching with the various contents of the metallic foil packages. We built the tag antenna on an actual metallic foil package and measured its performance, verifying that the proposed tag antenna can be used in item-level RFID applications for metallic foil-packaged goods at low cost.

### II. ANTENNA DESIGN AND OPTIMIZATION

Fig. 1 shows the overall geometry and design parameters of the proposed tag antenna, which is composed of a slot radiator and a feeding loop connected to a microchip. Both the slot and the feeding loop are etched onto a substrate of polyethylene (PET;  $\epsilon_r = 3.9$ ,  $\tan \delta = 0.003$ , thickness =  $50 \mu\text{m}$ ) for flexibility and to minimize cost. The measured input impedance of the tag chip (Impinj, Monza3) is  $20 - j170$  at 912 MHz, and the threshold power level of the tag chip ( $P_{chip \text{ min.}}$ ) is  $-15$  dBm. The small rectangular feeding loop is placed on top of the slot radiator, and the PET layers ( $H_1 = 50 \mu\text{m}$  and  $H_2 = 50 \mu\text{m}$ ) are filled between the loop feeder and the radiator as shown in Fig. 1(a). The design parameters for the tag antenna are perimeter ( $L_f \times W_f$ ),

Manuscript received August 30, 2010; revised May 05, 2011; accepted June 16, 2011. Date of publication September 19, 2011; date of current version January 05, 2012. This work was supported by the National Research Foundation of Korea Grant funded by the Korean Government (NRF-2010-013-D00055).

J. Ryoo is with the RFID Research Lab., LS Industrial Systems Co., Ltd., Gyeonggi-do 431-080, Korea (e-mail: jkryoo@lsls.biz).

J. Choo is with Department of Electrical Engineering, Korea Advanced Institute of Science and Technology (KAIST), Daejeon 305-701, Korea (e-mail: jychoo@kaist.ac.kr).

H. Choo is with the School of Electronic and Electrical Engineering, Hongik University, Seoul 121-791, Korea (e-mail: hschoo@hongik.ac.kr).

Digital Object Identifier 10.1109/TAP.2011.2167911

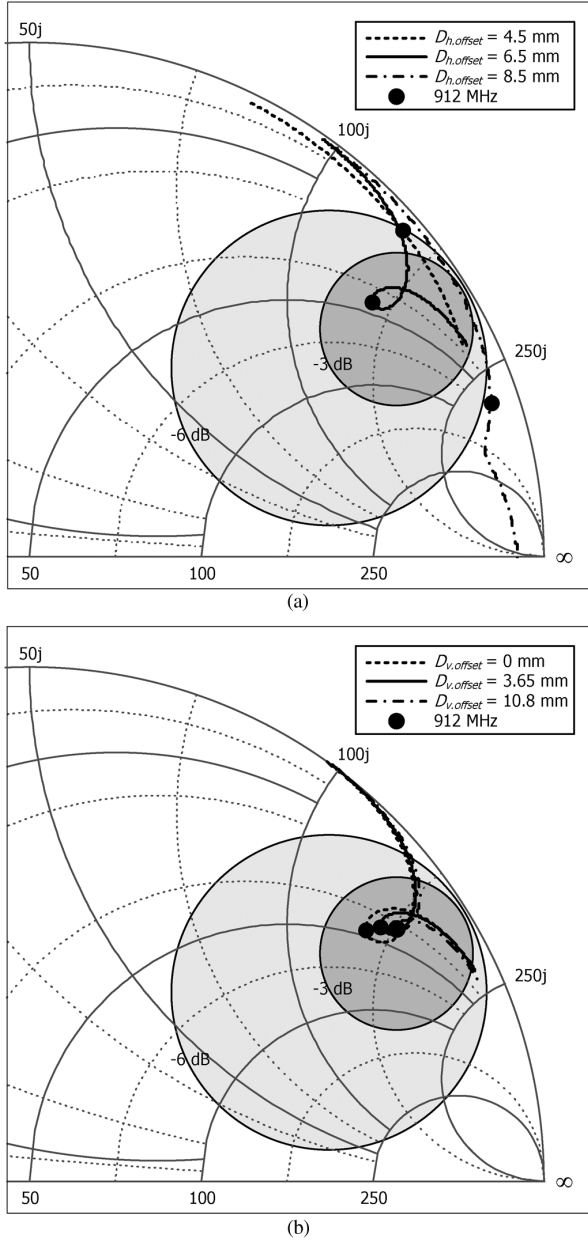


Fig. 2. Impedance on Smith chart: (a) varying  $D_{h.offset}$  at a fixed  $D_{v.offset} = 3.65$  mm. (b) varying  $D_{v.offset}$  at a fixed  $D_{h.offset} = 6.5$  mm.

line width ( $L_{lf}$ ,  $W_{lf}$ ), position ( $D_{h.offset}$ ,  $D_{v.offset}$ ), and slot size ( $L_s \times W_s$ ). The feeding loop, which resonates in combination with the capacitive microchip, induces currents on the surface of the slot by using proximity inductive coupling. The dimensions of the slot ( $L_s \times W_s$ ), the feeder loop ( $L_{lf}$ ,  $W_{lf}$ ,  $L_f \times W_f$ ), and the horizontal position of the loop ( $D_{h.offset}$ ) mainly determine the resonance frequency, while the vertical position of the loop ( $D_{v.offset}$ ) controls the quality factor (Q) of the antenna.

To interpret the impedance characteristic of the proposed antenna, we investigate the antenna impedance by using a commercial full-wave EM simulator (Ansoft HFSS) according to the position of the feeding loop. Fig. 2 shows the computed antenna impedance on a Smith chart, ranging from 612 MHz to 1,212 MHz, by varying the  $D_{h.offset}$  and  $D_{v.offset}$ , respectively. In the same figure, we added  $-3$  dB and  $-6$  dB received power coefficient locus to observe the impedance characteristics more easily. As  $D_{h.offset}$  increases at a fixed  $D_{v.offset}$  of 3.65 mm, the antenna impedance rotates in counterclockwise, as

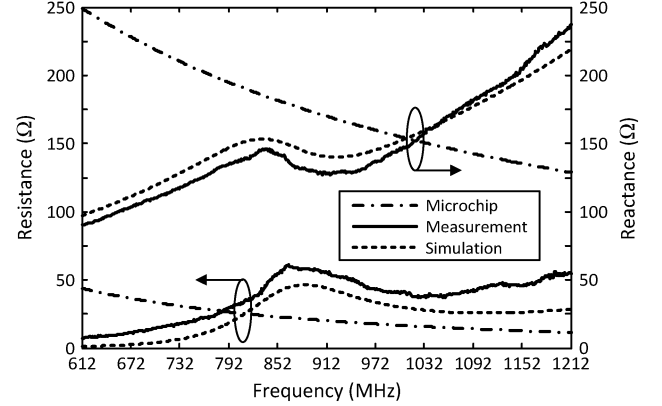


Fig. 3. Simulated and measured input impedance.

shown in Fig. 2(a), because  $D_{h.offset}$  changes the coupling coefficient between the slot and the loop feeder, similar to an inductively coupled antenna [8]. To make the antenna operate at the UHF RFID frequency used in South Korea, we used a  $D_{h.offset}$  of 6.5 mm when the input impedance of the tag chip is  $20 - j170$  at 912 MHz. We then change the value of  $D_{v.offset}$  as shown in Fig. 2(b). The impedance contour diameter of the  $\alpha$ -shape is changed according to the value of  $D_{v.offset}$ , resulting in variation in the quality factor (Q) and the bandwidth of the antenna. Based on the aforementioned parametric study, we obtain the optimized design parameters as follows:  $L_g = 200$  mm,  $W_g = 160$  mm,  $L_s = 116.4$  mm,  $W_s = 14.6$  mm,  $L_f = 11.3$  mm,  $W_f = 27$  mm,  $L_{lf} = 1$  mm, and  $W_{lf} = 3.7$  mm.

### III. RESULT

To verify the performance of the proposed tag experimentally, the input impedance of the fabricated antenna is measured by using a coaxial balun probe and an Agilent E5071C vector network analyzer. Fig. 3 represents the measured and simulated antenna impedance, as well as the conjugate impedance of the tag chip. The simulated impedance agrees well with the measurement, and their values are close to the conjugated chip impedance in the frequency range of interest. Particularly, the slope of the reactance curve appears to be parallel to that of the conjugated chip in the range of 860 MHz to 960 MHz, which results in broadband matching in the worldwide UHF RFID frequency band.

Fig. 4 shows the derived power reflection coefficient curves based on the measured chip impedance and both measured and simulated antenna impedances. In the same figure, we also added the measured read range conducted in an anechoic chamber. The simulated half-power bandwidth (power-reflection coefficient  $< -3$  dB) is 298 MHz (32.7%), from 798 MHz to 1,096 MHz and the measurement is 294 MHz (32.2%), from 799 MHz to 1,093 MHz. Such a broad bandwidth makes it applicable for used in various target materials with different dielectric constants. In addition to bandwidth, to examine the performance change depending on various target objects, we simulated the read range when 5-mm-thick dielectric materials were placed underneath the proposed tag antenna as shown in Fig. 5. The relative dielectric constant for the target changed from 1 to 9. Then the read range  $R_{tag}$  was calculated using (1) as follows, with the simulated radiation gain, impedance mismatch, and a reader with 36 dBm EIRP [9]:

$$R_{tag} = \frac{\lambda}{4\pi} \sqrt{\frac{P_{EIRP}}{P_{tag}}} = \frac{\lambda}{4\pi} \sqrt{\frac{P_{EIRP} (1 - \Gamma_{tag}^2) Eff_{tag} D_{tag}}{P_{chip min}}} \quad (1)$$

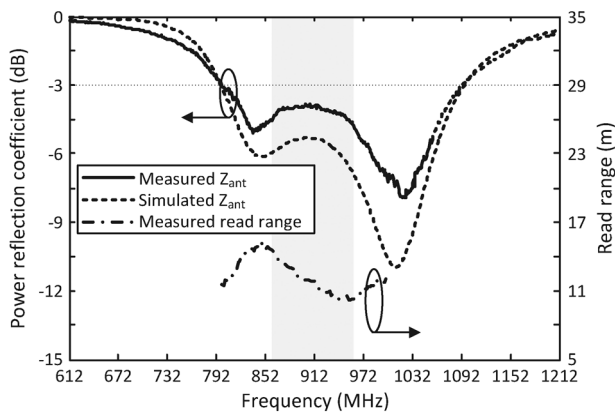


Fig. 4. Power-reflection coefficient of the proposed antenna.

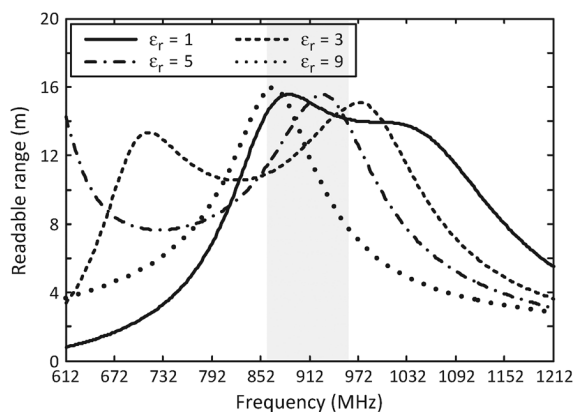


Fig. 5. Simulated read range by varying underlying materials.

where minimum operating power  $P_{tag}$  is expressed by the power-reflection coefficient  $\Gamma_{tag}$ , the radiation efficiency  $Ef_{tag}$  and the directivity  $D_{tag}$  of the proposed tag, and  $P_{EIRP}$  is the transmitting power of reader. Although there exist frequency shifts of maximum read range to the lower frequency band, good read range from 12 m to 15.1 m was observed at 912 MHz.

#### IV. CONCLUSION

We proposed a novel UHF RFID tag based on proximity inductively coupled feeding with the slot radiator for metallic foil packages. The fabricated tag antenna showed broad matching characteristics of 294 MHz (32.2%), from 799 MHz to 1,093 MHz. The measured reading distance was over 10 m at 36 dBm EIRP in the UHF RFID frequency band. The results verified that the proposed low-cost tag antenna can be used with a metallic foil package with various inner materials.

#### REFERENCES

- [1] C. Cho, H. Choo, and I. Park, "Design of planar RFID tag antenna for metallic objects," *Electron. Lett.*, vol. 44, no. 3, pp. 175–177, Jan. 2008.
- [2] S. Weigand, G. H. Huff, K. H. Pan, and J. T. Bernhard, "Analysis and design of broad-band single-layer rectangular U-slot microstrip patch antennas," *IEEE Trans. Antennas Propag.*, vol. 51, no. 3, pp. 457–468, Mar. 2003.
- [3] S. L. Chen and K. H. Lin, "A slim RFID tag antenna design for metallic object applications," *IEEE Antennas Wireless Propag. Lett.*, vol. 7, pp. 729–732, Nov. 2008.

- [4] L. Mo, H. Zhang, and H. Zhou, "Broadband UHF RFID tag antenna with a pair of U slots mountable on metallic objects," *Electron. Lett.*, vol. 44, no. 20, pp. 1173–1174, Sep. 2008.
- [5] X. Zeng, J. Siden, G. Wang, and H. E. Nilsson, "Slots in metallic label as RFID tag antenna," in *Proc. IEEE Antennas and Propagation Society Int. Symp.*, Jun. 2007, pp. 1749–1752.
- [6] L. Ukkonen, M. Schaffath, L. Sydanheimo, and M. Kivikoski, "Analysis of integrated slot-type tag antennas for passive UHF RFID," in *Proc. IEEE Antenna and Propagation Society Int. Symp.*, Jul. 2006, pp. 1343–1346.
- [7] K. H. Lin, S.-L. Chen, and R. Mittra, "A capacitively coupling multi-feed slot antenna for metallic RFID tag design," *IEEE Antennas Wireless Propag. Lett.*, vol. 9, pp. 447–450, Apr. 2010.
- [8] H. Choo and H. Ling, "Design of electrically small planar antennas using inductively coupled feed," *Electron. Lett.*, vol. 39, no. 22, pp. 1563–1565, Oct. 2003.
- [9] P. V. Nikitin and K. V. S. Rao, "LabVIEW-based UHF RFID tag test and measurement system," *IEEE Trans. Ind. Electron.*, vol. 56, no. 7, pp. 2374–2381, Jul. 2009.

### Design of a Broadband All-Textile Slotted PIFA

Ping Jack Soh, Guy A. E Vandenbosch, Soo Liam Ooi, and Nurul Husna Mohd Rais

**Abstract**—A new broadband textile based PIFA antenna structure designed for wireless body area network (WBAN) applications is presented. The new topology can be directly integrated into clothing. The study starts by considering three different materials: flexible copper foil, and ShieldIt Super and pure copper polyester taffeta conductive textiles. Bandwidth broadening is successfully achieved by implementing a novel and simple slot in the radiating patch. The measured reflection coefficient and radiation characteristics agree well with simulations. Moreover, radiation characteristics and bandwidth show satisfactory immunity against detuning when operating on-body, especially when placed on the back. To our knowledge, the proposed structure is the first fully fabric based slotted PIFA to be reported in open literature with high bandwidth (more than 46%) and reasonable gain (ca. 1.5 dB), to be used for multiple applications in the frequency band of 1.8 to 3.0 GHz.

**Index Terms**—Broadband antennas, conformal antennas, planar inverted-f antennas (PIFA), textile antennas.

#### I. INTRODUCTION

Due to the increasing demand for multi-functional, multi-band wireless operation and consumer-centric technology, textile antennas have

Manuscript received October 05, 2010; revised May 20, 2011; accepted July 15, 2011. Date of publication September 15, 2011; date of current version January 05, 2012. This work was supported in part by the Malaysian Ministry of Higher Education (MOHE).

P. J. Soh is with the Telecommunications & Microwave Research Division, Department of Electrical Engineering (ESAT-TELEMIC), Katholieke Universiteit Leuven, 3001 Leuven, Belgium, on leave from the School of Computer and Communication, Universiti Malaysia Perlis (UniMAP), 02000 Kuala Perlis, Malaysia (e-mail: pingjack.soh@esat.kuleuven.be).

G. A. E. Vandenbosch is with the ESAT-TELEMIC, Katholieke Universiteit Leuven, 3001 Heverlee, Belgium (e-mail: guy.vandenbosch@esat.kuleuven.be).

S. L. Ooi and N. H. M. Rais are with the School of Computer and Communication Engineering, Universiti Malaysia Perlis (UniMAP), 02000 Kuala Perlis, Malaysia (e-mail: sooliam@gmail.com; nwhosena@gmail.com).

Color versions of one or more of the figures in this communication are available online at <http://ieeexplore.ieee.org>.

Digital Object Identifier 10.1109/TAP.2011.2167950